123

Towards a micromechanic understanding of the pressure distribution under heaps

Hans-Georg Mattutis[1], Alexander Schinner[2], Tetsuo Akiyama[4], Junya Aoki[4], Satoshi Takahashi[4], Keiko M. Aoki[3], Klaus Kassner[2]

[1] Department of Applied Physics, School of Engineering,The University of Tokyo, Bunkyo-ku, Tokyo 113, Japan

[2] Otto-von-Guericke-University Magdeburg, Universitätsplatz 2,D-39016 Magdeburg, Germany

[3] JST, nano-LC project, TRC, Tokodai 5-9-9, Tsukuba 300-2635, JAPAN

[4] Department of Chemical Engineering, Shizuoka University, Hamamatsu, 432, Japan

Abstract

The pressure distribution under heaps has found to be dependent on the building history of the heap both in experiments and in simulations. Up to now, theoretical models and analysis assume that the packing of the heap is homogeneous. We show new experimental and simulational results which indicate that the packing is inhomogeneous and that this packing property is likely causing the pressure minimum under the heap.

1   Introduction

In recent years, the rather unintuitive existence of a pressure minimum under granular heaps created some excitement in the physics community involved in granular research[1, 2, 3], as the phenomenon was considered to be a special paradigm of granular materials. This triggered the publication of a review on the problem[4]

Figure 1: Possible construction history of heaps.

which showed that the pressure distribution under granular heaps is a long standing topic in granular research and not in all experiments a pressure dip was observed. Heaps with[5, 6, 7, 8] and without[9, 10] pressure minimum in the middle have been reported in the literature. Experiments showing a pressure dip could usually be found in the chemical engineering literature, whereas the heaps without pressure dip were predominant in the context of civil engineering. This was interpreted by one of the authors (H.-G. M. in Ref. [11]) as an effect of the construction history. This was corroborated by molecular dynamics simulations[11], which have recently been verified experimentally[12]. Wedge sequences, where the heap is poured from a point source, should exhibit a pressure minimum, in contrast to layered sequences, where the particles are rained uniformly onto the heap (for the terminology of the construction history, see Fig. 1). Theoretical insight in physics results only if the correspondence between theory and experiment is clear. Because the phenomenology of the pressure distribution is rather complicated, in this paper, we want to focus on a micromechanic investigation of the outcome for the pressure distribution.
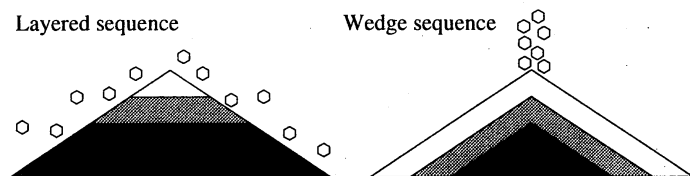
1.1 Arching

The first arches which where built into a "granular heap" where the tomb chambers in Egyptian pyramids. The pyramids internal structure, see Fig. 2, reminds to the stress model given in Ref. [2]. After "false arches" in Egypt and ancient Greece, "true arches" were discovered as a principle in civil engineering by the Romans, and with little modifications as Gothic arches, the concept is prevalent till today. Arching as a topic in granular materials is a comparatively new concept, dating back not much more than hundred years. The first references on a mathematical treatment of "Bogenbildung" (arching) in Terzaghi's textbook on "Erdbaumechanik" (geotechnics) [13] go back to the last quarter of the nineteenth century[14, 15]. Arching as a "prime suspect" for the formation of the pressure dip was already mentioned in the experimental papers on the pressure dip[6].
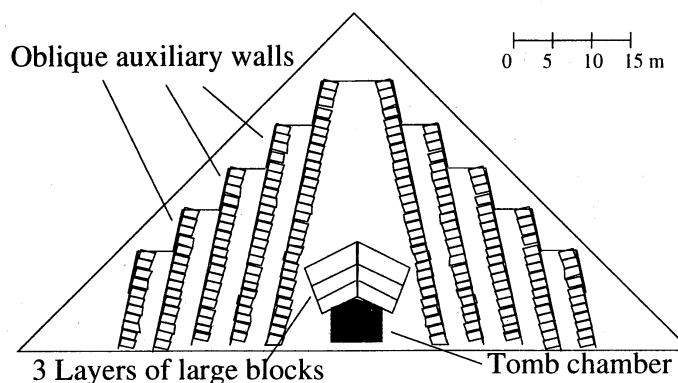
Figure 2: Crossection of the pyramid of Pharao Sahure (dated about 2500 B.C.) at Abu Sir. The building method is not homogeneous, but consists of horizontal masonry, inclined walls to direct the pressure out of the middle, and large blocks which form a "false arch" above the tomb chamber. Usually, the "angle of repose" in pyramids is 56 degrees.

1.2 Phenomenology of arching under granular heaps

The ability to predict when and why arching occurs is still very rudimentary. The granular cone built from a point source in Ref. [5] exhibited a distinct pressure minimum, whereas for the wedge in the same reference the pressure dip was negligible. Also in other references[9, 10] granular wedges exhibited no pressure minima. The granular cones built from a point source in Ref. [6] showed a distinct minimum for polydisperse glass beads of different sizes and sand, but for the nearly monodisperse rape seed, the pressure dip almost vanished. The results by Smid and Novosad [7] which largely triggered the excitement about the granular research,
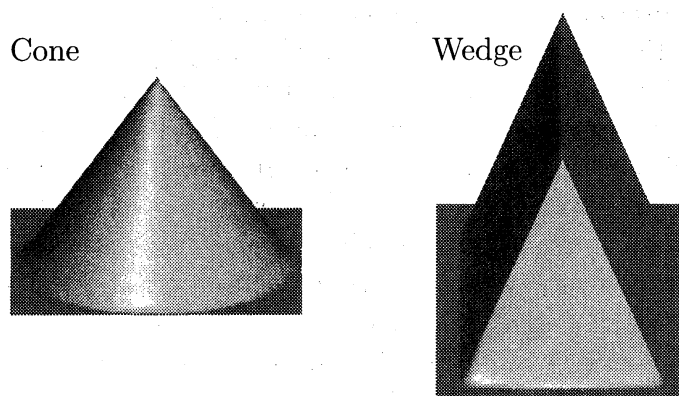
Figure 3: Granular cones and granular wedges

showed nearly scalable results for sand and granular fertilizer for different heap sizes, but as both materials are composed of rough, polydisperse grains, this could rather be expected. Ref. [8] used the widest range of different materials for cones built in a wedge sequence, ranging from sand over small and large monodisperse glassbeads. Polydisperse materials turned out to always yield a pressure minimum. Monodisperse smooth large glass beads exhibited no pressure minimum, but small monodisperse and frosted large glass beads showed a pressure dip. This was a crucial finding, as the size of the particles and their surface properties seemed to influence the resulting pressure distribution. The small monodisperse glass beads were of a size (< 0.4 mm) so one had to suspect effects of cohesion. Finally, the effect of the construction history was verified experimentally in Ref.[12], where wedge sequences showed a pressure dip in wedges and cones, whereas layered sequences showed a pressure dip neither in wedges nor in cones.
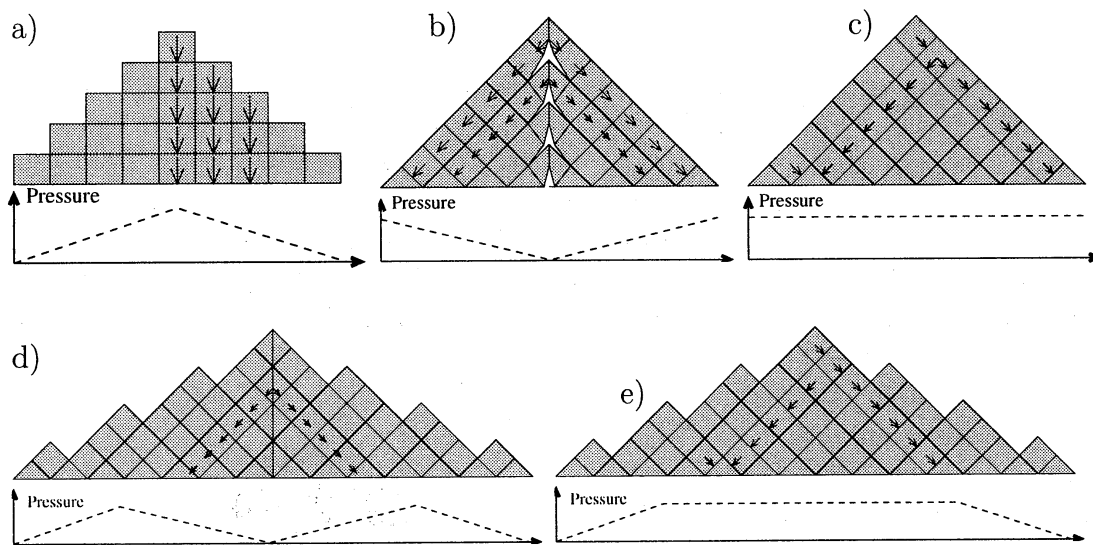
Figure 4: "Generic" models for the pressure distribution under a heap in a) to c) and manipulation of the angle of repose in a "generic" model in d), e).

1.3 Why we don't use "theory" (yet)

Because many physical properties of the grains seem to influence the forming of a heap, we refrained from the use of macroscopic models or from using simple computational models, where several quantities have to be absorbed in a single parameter. In physical sciences, "generic" models are usually used for the fundamental understanding of physical processes. Of course one can set up "generic" models for the pressure distributions with pressure maxima or flat curves in the middle of the heap, see Fig. 4. The generic models correspond then to averaging of representative volumes composed of many grains ("mean field approximation" in Ref. [2]). Whether one uses a discrete model (as in Fig. 4) or partial differential equations does not make much difference. In both cases, the outcome of the calculation has been intrinsically determined by the choice of of the model. The "brick-model" in Fig. 4 a) has a pressure maximum in the middle. The "arching-model" in Fig. 4 b) is similar to the solution in Ref. [2].

The "flat model" in Fig. 4 c) corresponds to the solution in Ref. [16], where monodisperse rounded particles are ordered on a hexagonal grid. The angle of the arches can be introduced as an additional parameter together with the angle of repose. The critical angle can then be manipulated, so that vanishing pressure at the sides of the heaps is obtained in Fig. 4d), e). Of course, such a phenomenological methodology allows the superposition of all three pressure distributions and the "reproduction" of any experimental outcome. Nevertheless, the models are only descriptive, they lack the power to predict the outcome of a given experiment with a given material, considering that experiments with and without pressure minimum have been reported. Also models for the pressure distribution like the one given in [6], where one half of the system was fitted to a double-peak structure, lack predictive power as to where and why a pressure dip occurs.

1.4   Problem outline

A better understanding of the formation of the pressure minimum requires studies on the micromechanic level. This includes the role of e.g. force network, friction, particle shape and roughness, size dispersion, packing density etc. Up to now, neither from the simulations nor from the experiments a complete consistent picture evolved as to what constitutes the exact mechanism for the formation of the pressure minimum. Therefore, we chose to investigate the problem with combined simulational and experimental methods to obtain insights beyond the current theoretical and experimental investigations.

Whereas it is now established that the the pressure minimum is caused by the wedge-sequence building history of the heap, it is not clear how the information about this history is stored. Possible mechanisms can be imagined as loading of normal contacts between grains, the mobilization of static friction in the tangential direction, packing densities, structure of the force network and so on. Before we address these questions, we want to clarify some points which are still ambiguous in the existing experimental literature[5, 6, 7, 8, 9, 10], at least on the micromechanic level.
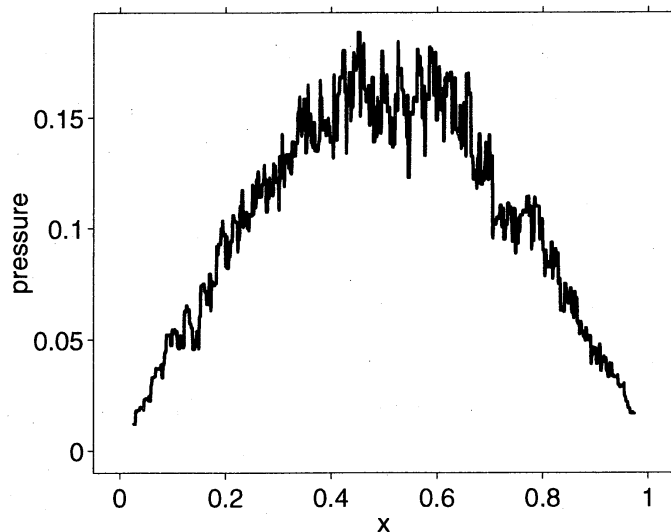

Figure 5: Pressure distribution for a simulation of monodisperse round particles (less than 8 % deviation in diameter) under a heap set up in a layered sequence.

Because the pressure minimum is well established for single heaps, we abstained from looking for the dip as a result of a configuration average of otherwise noisy data like in Ref. [17]. The dip should be pronounced even for a single configuration, both in the experiment and in the simulation.

1.5   Setup of the simulations and experiments

Granular cones and granular wedges built in a wedge sequence exhibit similar behavior[12]. Therefore, we considered that the computational treatment in two dimensions was sufficient to understand the microstructure of the heap.

To simplify the investigation, we assume that the bottom of the heap is neither deformed by external mechanism, neither by bending like in Ref. [18] or compression along the x-axis like in Ref. [17]. This is certainly the case for the setups used in [6, 8, 12] and for our own experiments. For the simulation, we choose not to fix the outermost particles, like in all the experiments we cited, in contrast to computational investigations like Ref. [19].

If not otherwise noted, all heaps in the experiments and simulations are built in a wedge-sequence, the grains are poured from a point source. All heaps are constructed on a flat ground, i.e. a ground without any surface asperities. In the simulations, the Young's modulus of the ground is the same as for the grains and the friction coefficient between ground and particles is the same as between the grains to simplify matters.

The setup of the experiments is described in appendix A, the simulation method is described in appendix B. For all graphs, experiment and simulation, the ground pressures are given in dimensionless units by rescaling the bottom pressure with 1/(g*height*density). Because the experimental pressure measurements used pressure gauges at different points, we graphed the results using point symbols. The "measurements" in the simulation have been made using "moving averages". As these can be computed for any position of the line element, we drew the pressures with continuous lines.

2   Grain properties for pressure dips

Because in the literature a variety of materials and setups has been used for the investigation of the pressure under heaps, ranging from rape seed over fertilizer, sand to glass beads, we first wanted to investigate which grain properties are necessary requirements for the formation of the pressure dip.

2.1   Monodisperse particles and layered sequence

For heaps of monodisperse smooth grains in the absence of cohesion, no pressure minimum in the middle is observed. For this situation, the calculation in Ref. [16], gives constant pressure in the middle, which describes the system quite well. The length of the zone with constant pressure depends on the angle of repose. This is because particles order on a

Figure 6: Stresses for for the simulation in Fig. 5 together with the outline of the heap.

triangular lattice and the pressure is propagated along the normal directions of the particles, like in Fig. 4 e). The simulation results are given in Fig. 5. It is possible to imagine a pressure dip in this figure, but, as the dip is smaller than the fluctuations, we consider
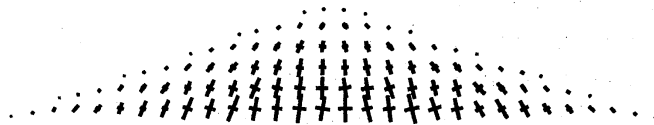
it not significant, in consideration of the experimental and computational results we will show later on. The histogram of the contact angles is given in Fig. 14b). The preference for ordering on a hexagonal grid is clearly obvious from the preferred contact direction along 60-degree axes. For monodisperse rounded particles with friction on a smooth surface, the difference in the pressure distribution to a system set up on an ordered grid[20, 21] without friction on a fixed base are negligible. We can also compute the stresses inside the heap after Ref. [22], see Fig. 6 (for volumes of about 10 × 10 particles), but the results for stresses and the comparison with analytical theories will be given in a later publication.

2.2 Artifacts for smooth particles

For a wedge sequence for monodisperse, not too smooth particles, the results for wedge sequences are the same as for layered sequences. If the particles are very smooth (many edges, in case of polygons), the aggregate of rounded particles is not able to withstand strong shear forces along the hexagonal crystal axes. This is true even in the presence of static friction, because the particles can escape the tangential friction
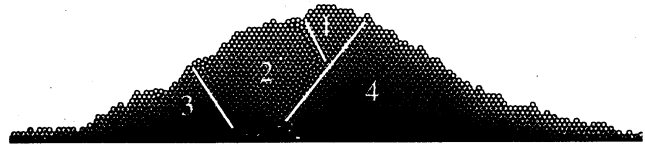

Figure 7: Deformed pile of exactly monodisperse round particles. For exactly monodisperse round particles, the pile is not triangular any more, but shaped rather like a Gaussian. The structure is polycrystalline, the monocrystals are denoted by white lines near, not at the fault lines.
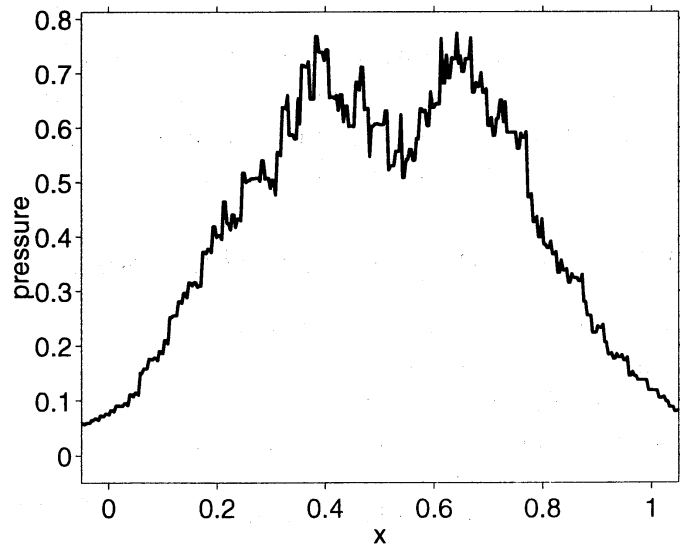
forces by rotation. Therefore, an aggregate of closest packing regions is realized.

Because the dynamics is not a dominated by avalanches and single particles any more, but by the movement of crystal boundaries in a polycrystalline aggregate, the pressure distribution is rather unpredictable. The heap will be not of triangular shape any more, but rather of a Gaussian shape (Fig. 7). For the crippled heap in Fig. 7, the pressure distribution accidentally exhibited a minimum (Fig. 8). (Other runs for the sample particle parameters did not necessarily exhibit a pressure minimum.) This pressure minimum is not an intrinsic "granular" property but due to the fact that the heap consists of four crystal regions, denoted by 1,2,3,4 in Fig. 7), where the regions 1,2 in the middle push out the wedges 3,4 at the sides.

Figure 8: Pressure under the deformed pile of monodisperse round particles in Fig. 7.

2.3 Effect of bottom rough

One of the more puzzling experimental results in the experiments in Ref. [8] is the fact that for monodisperse small glass beads (180 μm diameter) a pressure minimum exists, but not for monodisperse large beads (560 μm diameter). The pressure dip for small glass beads seems also to contradict simulation results[11], and the experimental rape seed pressure distributions in [6], where the pressure dip for "nearly" monodisperse systems practically vanishes.

As the experiment in Ref. [8] does not use the standard circular pressure gauges with smooth metallic surfaces, first we investigated whether we could obtain a pressure dip with small ($< 560\mu$m diameter) monodisperse particles in the standard setup with smooth metallic pressure gauges comparable to the ones used in Ref. [6, 7, 9, 10].

As can be seen from Fig. 9, for monodisperse particles of about 230 μm diameter the pressure dip is well developed, whereas for monodisperse particles of about 463 μm diameter in Fig. 10 no pressure dip exists.

In contrast to nearly monodisperse particles, for particles of about 460 μm particle diameter and a deviation of the particle radius of up to a factor of 3.3, the pressure dip for glass beads is already well developed, as can be seen from Fig. 11.

Generally, in our experiments with smooth bottom and smooth metallic pressure gauges, the fluctuations are stronger in comparison to Ref. [8]. The bottom roughness seems to stabilize the pressure distribution and to reduce the fluctuations.
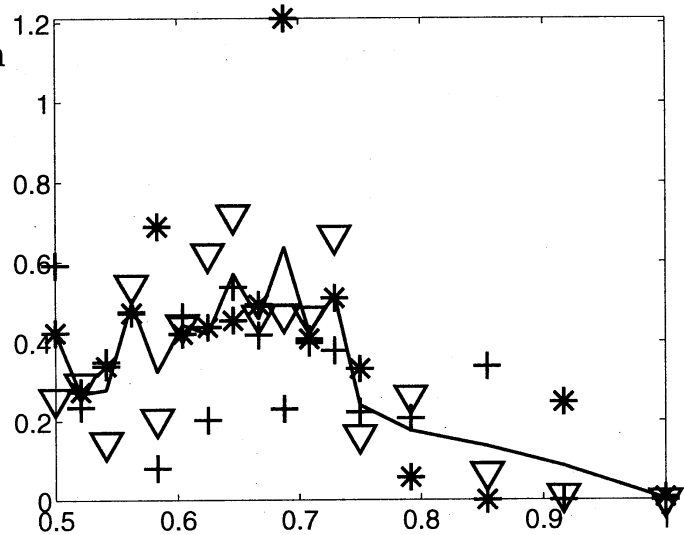

Figure 9: Pressure distribution for small glass beads and an average grain diameter of about 230 μm diameter, monodisperse (210-250 μm). Three different measurements at the same position, the line is drawn through the average of the dots to guide the eye.
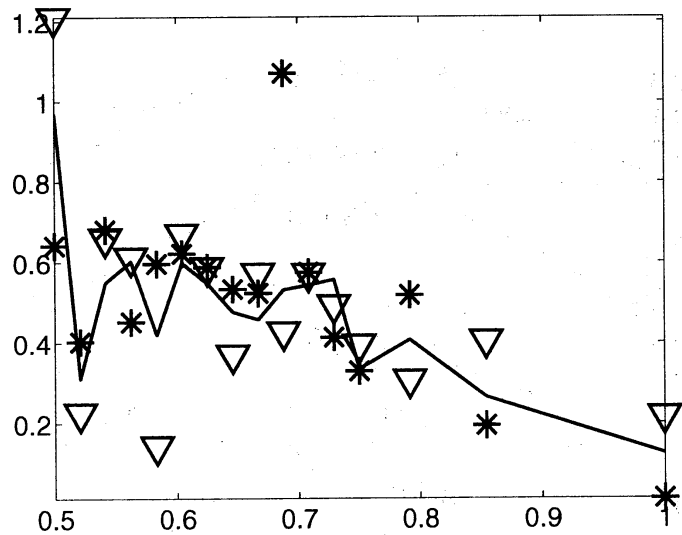

Figure 10: Pressure distribution for glass beads with 463 μm average diameter, monodisperse (425-500 μm). Two different measurements at the same position, the line is drawn through the average of the dots to guide the eye.

2.4 Effect of cohesion and particle roughness

From the previous section, we can assume that the pressure dip for particles below 180 μm diameter in Ref. [8] were not caused by some polydispersity on the micrometer scale. The pressure dip seems to occurs only for glass bead with grain diameters below 460 μm. For dry granular materials "scalability" can be assumed, i.e. for moderate rescaling (below the yield stress of the single grains) of the system size the physical properties like pressure distribution and so on will not change. Cohesion due to the humidity in the surrounding air introduces a new length scale which violates these scaling properties for particles which are small small enough. In Ref. [11], where non-cohesive particles have been investigated via computer simulations, only polydisperse systems exhibited a pressure minimum.
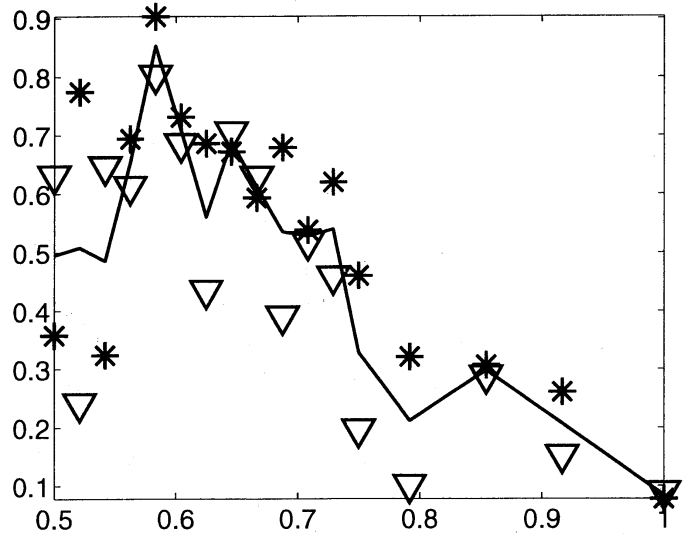

Figure 11: Pressure distribution for glass beads and an average grain diameter of about 460 μm diameter and large polydispersity (210–710 μm). Two different measurements at the same position, the line is drawn through the average of the dots to guide the eye.
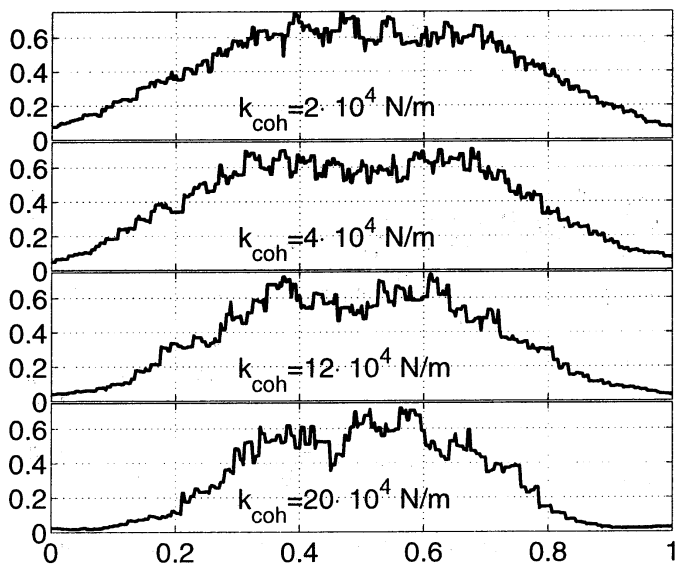

Figure 12: Pressure distribution under heaps for simulations of monodisperse particles (7 corners) and different cohesion strength. The pressure dip develops with increasing cohesion.

In contrast, cohesion changes the movement of grains from single particles to clusters of correlated particles. This was conjectured by experiments in Ref. [23, 24]. A micromechanic investigation by computer simulations in Ref. [25, 26] corroborated this picture. From the non-uniformity of the cohesive force results a disorder of the packing and a polydisperse mixture of clusters. Therefore, a system with monodisperse cohesive particles behaves effectively like a system of polydisperse particles. In Fig. 12, the increase of the pressure dip for increasing cohesion strength is shown. Nevertheless, not only the pressure minimum, but also the fluctuations increase, so it is debatable whether the "dip" leftward of the middle of the heap in the lowest graph of Fig. 12 is not actually a large fluctuation. In some cases, for very strong cohesion, two minima

develop. The interpretation that cohesion affected the system for particles with 230 μm diameter is consistent with the fact that the bulk density for these small beads was 1.579g/cm^3, which was definitely smaller than the bulk density of the other glass beads (see Tab. 1). As the cohesion inhibits the compaction, therefore leading do smaller densities, could already be observed by previous simulations[25, 26].

The influence of the humidity of the surrounding air on granular materials has been investigated already in Ref. [27], where the static friction has been observed to show a time dependence. Because it is nearly impossible to perform "absolute dry experiments" because of static electricity, we performed instead simulations of monodisperse particles with cohesion. The algorithms are described in Ref. [25, 26]. As can be seen in Fig. 12, for increasing cohesion strength the dip increases, which can be attributed to the increased effective polydispersity of the clusters made up from single particles.

In some experiments in powder technology like in the Hosokawa powder tester (as proposed by Carr [28]), the strength of the cohesion and the surface roughness of the particles is classified by a single parameter, the flowability. This flowability seems to be responsible why a system with 460 μm diameter glass beads and less than 8 % deviation (Fig. 10) in diameter behaves is a monodisperse system and exhibits no pressure dip, whereas sand with the same diameter and size dispersion shows a pressure dip (Fig. 13). For the same reason, the monodisperse frosted glass beads in Ref.[8] with about 1 mm diameter diameter showed a pressure minimum. Analogously, in a computer simulation a system composed of monodisperse rough or elongated particles can show a pressure dip, because reordering for rough and elongated particles due to geometric constraints is more difficult than for smooth and round particles. Macroscopically this has been observed in computer simulations as a higher yield stress -for smooth elliptic particles in comparison to smooth round particles[29].
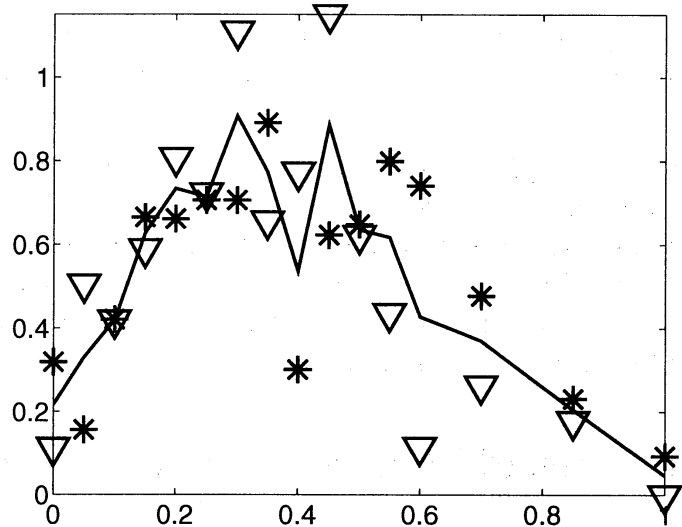
Figure 13: Pressure distribution for sand with 463 μm average diameter, monodisperse (425-500 μm). Two different realizations of the same measurement, the line is drawn through the average of the dots to guide the eye.

2.5 Distribution of the contact angles

The distribution of contact angles is strongly influenced by the geometry of the particles. For nearly monodisperse particles (less than 2 % deviation in diameter), the possible effect on the pressure distribution was described in section 2.1. In this case, the probability for contact angles is strongly peaked near the values of the triangular grid, see Fig. 14 a). For more polydisperse particles (up to 25 % deviation in diameter), the peaks for the

(a) rounded particles, monodisperse

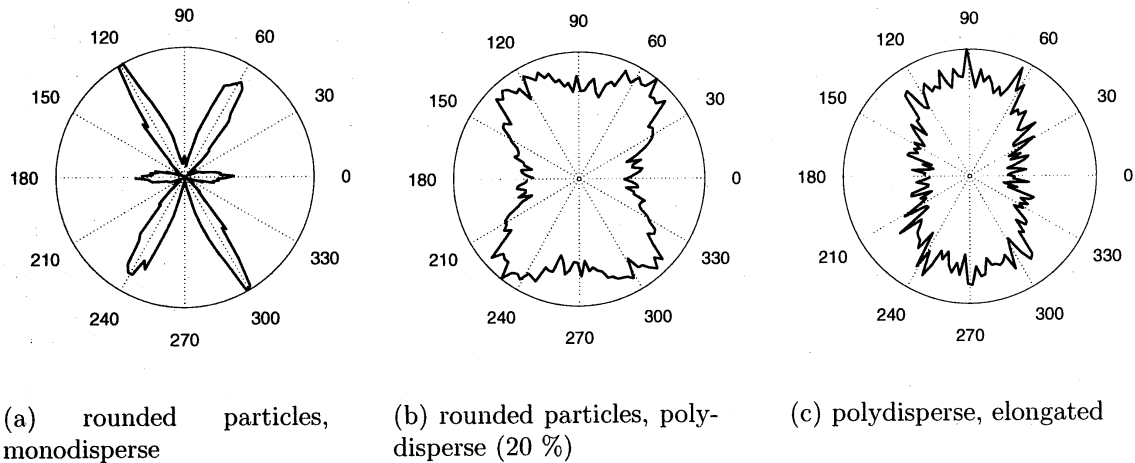(b) rounded particles, polydisperse (20 %)

(c) polydisperse, elongated

Figure 14: Histogram of the angle of the particle contacts versus the horizontal axis. Graphs a) and c) are for wedge sequences, graph b) is for layered sequence.

triangular grid are still recognizable, but are already strongly smeared out, see Fig. 14 b). For a size distribution of more than a factor of two, no structure is recognizable any more in the distribution of the contact angles, though the directions along the triangular grid are still favored see Fig. 14 c). As a rule of thumb one can say that long as the angle distribution is peaked around the angles of the hexagonal grid, in general no pressure dip is found in the configurations.

3 Detailed Investigation of the heap structure

3.1 Force network

Force networks enjoy a certain popularity under theoretical physicist due to their similarity to random walks, fractals and other geometric paradigm of theoretical physics. Nevertheless, we were not able to extract any meaningful informations from force networks as given in Fig. 15, though the corresponding pressure distribution shows a rather clear minimum.

3.2 Density of the heap

The experimental findings of the previous sections indicate that the pressure minimum is a rather stable phenomenon. Perturbations like the rebuilding of the heap or the removal of an inserted rod seem only to broaden the pressure dip. Even under vibration for certain grain types the pressure dip does not vanish totally. In simulations, the pressure minimum seems to be ingrained in the heap on a level that vibration amplitudes of the order of the inter-particle penetration depth cannot destroy it easily. Therefore we looked for a more macroscopic effect, instead of microscopic contact loading etc. The data of contact network proved to be inconclusive: Due to the noisiness, we would not devise any meaningful structure or statistics.
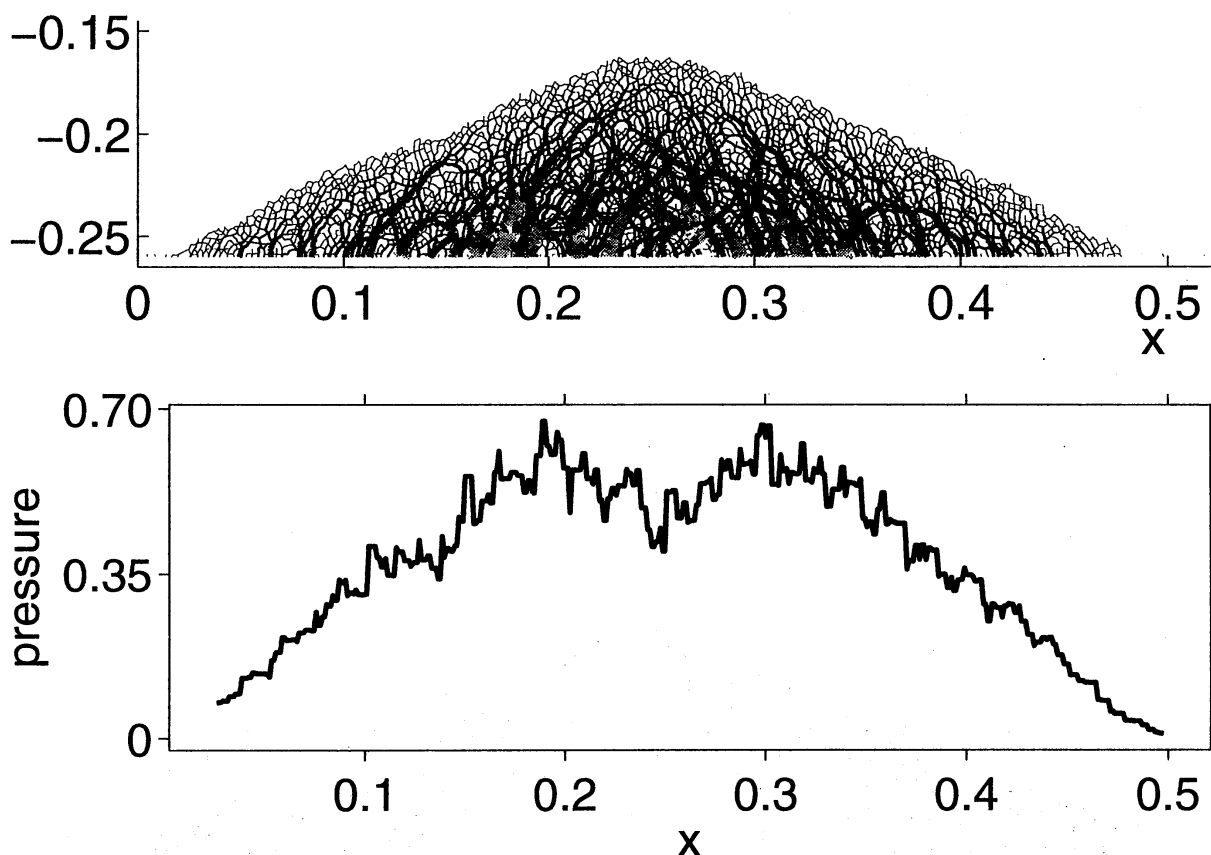
Figure 15: Force network (middle) inside a heap with polydisperse particles built from a wedge sequence and the corresponding bottom pressure distribution (below). Stronger forces are denoted by broader and lighter lines.

One possibility is that the heap was not homogeneous. By plotting the averaged density of the heap (Fig. 17) for heaps which gave an averaged pressure dip (Fig. 16), we found that the middle region exhibits higher density than the rest of the heap. This core of higher bulk density existed for all heaps that showed a pressure minimum in the middle. It seems to be this core of high bulk density which forms under the impact of the grains in the wedge sequence and the shearing due to the resulting avalanches which forms the core of the "arch" which results in the pressure dip. Another interesting feature of the pressure distribution Fig. 16 for various heights is that the pressure distribution changed with the relative height inside the heap, in contrast to assumptions/ predictions in the literature[1, 2, 3]. The pressure in the highest layer does not exhibit a pressure minimum at all, which is consistent with the fact that the highest layer of nearly the width of the channel of impacting particles is a layered sequence from the point of the construction history rather than a wedge sequence.

We had no facility to investigate experimentally the density of the heaps, but the computational density deviations with a "funnel" of about 8 % higher density in the
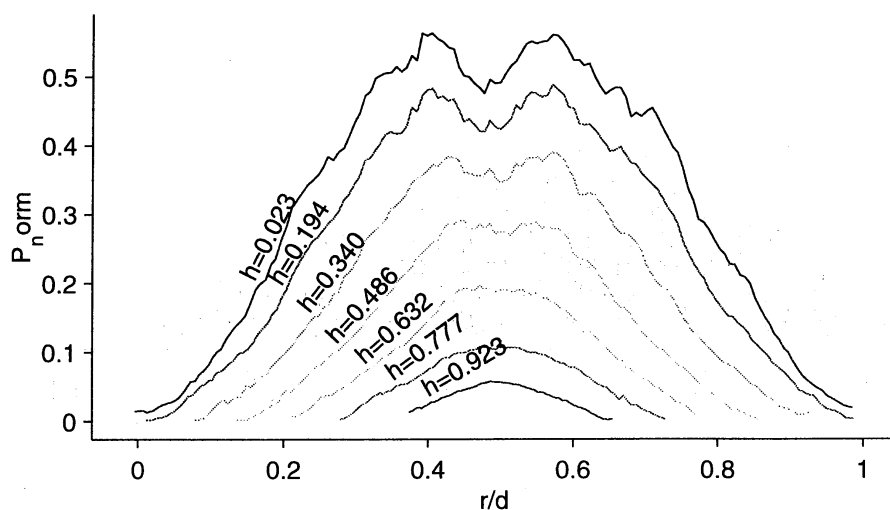
134

Figure 16: Pressure distribution averaged from 10 heaps with polydisperse particle size distribution and wedge sequence. The pressure is measured at various heights and the curve does not scale for pressures in higher regions.
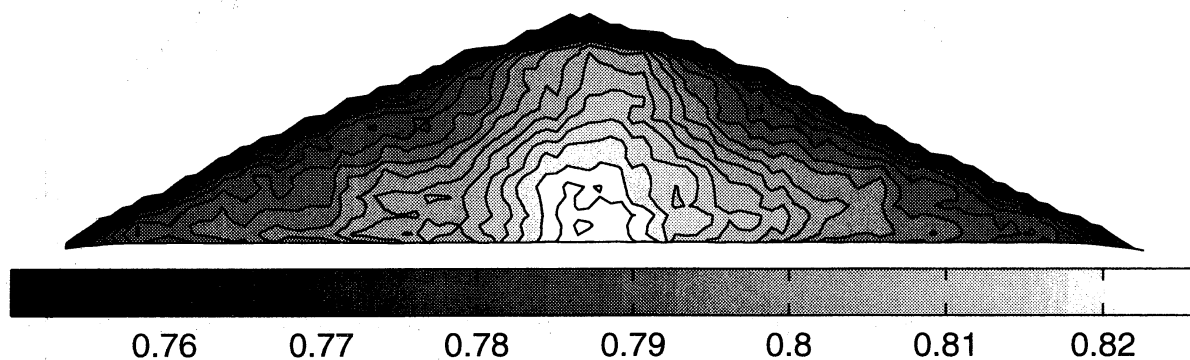

Figure 17: Bulk density averaged from the 10 heaps of Fig. 16.

middle of the pile correspond reasonably well with the increased bulk density in the packing distribution of a Catalyst bed filled from a point source in Ref. [30]. We did not find any significant density differences for the heap build in a layered sequence, and for such a "rainy" uniform filling method, also experimentally no density differences were observed in Ref. [30].

4 Conclusions

We have shown experimental and computational evidence that for heaps with a pressure dip in the middle the density is not homogeneous, but depends both on the building process and the material used, which both affect the width and the depth of the pressure dip. Micromechanically, a necessary requirement for the occurrence of a pressure dip under a heap seems to be that in the construction history, the homogeneity of the pile is broken. As shown, this could be accomplished either by piling the heap from a point

source directly or by piling the heap around a central object. Further, it is necessary that the grains allow that the inhomogeneous density is unaffected by impacting particles. This is only possible if the reordering is prohibited due to geometrical effects or other contact forces. For the buildup of a heap, this results automatically in a region of (up to 10 %) higher bulk density than in the outlying regions. This region determines the size the higher density, which corresponds to the width of the arch, below which the pressure is reduced with respect to the maximum pressure under the heap.
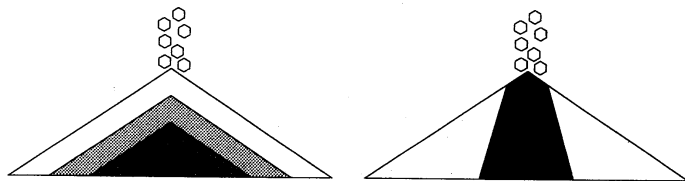

Figure 18: Sketch of the building history of the wedge sequence (left, older regions are darker) and the density profile of the wedge sequence (right, region with higher bulk density is darker).

As kinematic constraints which inhibit the reorganization into a more homogeneous configuration either size polydispersity, shape polydispersity or reduced "flowability" by high surface roughness (sand instead of glass beads, as in our case, or frosted glass beads like in Ref. [8]) or cohesion (for small particles $< 400\mu$m diameter, the humidity of the surrounding air seems to be sufficient). This density distribution, sustained by the above granular properties, creates the arch which is responsible for a reduced force propagation into the middle of the heap, which creates the pressure dip. It is therefore possible to interpret the pressure dip under heaps as a "macroscopic" phenomenon (texture inhomogeneities inside the heap of the size of the heap dimensions), and it is not necessary to resort to interpretations on a more microscopical level (loading or mobilization of friction on length scales of the order of the particle contact areas). For the arching situation, the pressure distribution resembles the one in Fig. 4b), whereas for the homogeneous heap, the situation is similar to Fig. 4c). Static friction is only a necessary condition which allows heaping on a flat surface, as we have seen that in the monodisperse system with rounded frictional particles no pressure minimum occurs, because grains can "escape" the friction via rotation. Disorder alone is not sufficient for the formation of a pressure dip, because disorder is also present in layered heaps without pressure dip. Nevertheless it is a necessary condition to hinder the reordering of the particle configurations.

It is certainly worthwhile to reconsider, whether it makes sense to investigate stresses in an obviously history-dependent and therefore timedependent system with time independent equations, as has has been done in the past[1, 2, 3]. Likewise, the homogeneity and isotropy depend on the history and lead to a much more varied phenomenology than had been anticipated by many theoretical works.

Due to the density differences inside the heap, it seems that computing the total mass of the heap by integrating the pressure distribution will probably lead to different results than by determining the bulk density in a test volume and than computing the weight of the heap by its geometric dimensions.

material	Glass beads				Sand
averaged diameter	230	460	463	655	463
diameter range	210-250	210-710	425-500	600-710	425-500
bulk density	1.579	1.675	1.609	1.644	1.506

Table 1: Materials used for the pressure measurements. The average diameter and the diameter are given in [μm], the bulk density is measured in [g/cm^3].

Acknowledgments

Appendix A: Experiments

The heap was constructed using a hopper with an outlet of 6.2 mm which was located 117 mm above the ground plate, see Fig. 19. The experiments have been performed on stainless steel ground plates of thickness 4.5 mm with pressure gauges of 12 mm diameter. 5 different plates (355 × 510 mm) have been
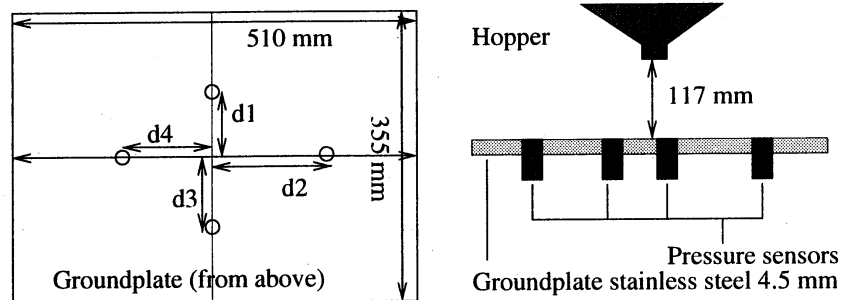

Figure 19: Experimental setup for the determination of the ground pressure.

used where 4 or 5 holes were drilled in different distances from the center, with a shift in the direction so to not interfere with each other. The distances d1, d2, d3, d4, d5 were for plate 1 were 0, 50, 70, 180, 200 mm, for plate 2 were 5, 30, 55, 165 mm, for plate 3 were 10, 40, 45, 120 mm, for plate 4 were 15, 35, 60, 85 mm and for plate 5 were 20, 25, 100, 140 mm. The material properties of the grains are given in Tab. 1.

Appendix B: Simulation Method

To model and numerically simulate cohesion as a feature of the contacts, we used the discrete element method. It is based on molecular dynamics, where the particle trajectories are computed according to Newton's equation of motion. The particles are represented by polygons. The force between two particles $\{i, j\}$ is proportional to the Young's modulus and to the overlap area (representing the deformation) of two polygons.

The contact geometry is sketched in Fig. 20. The friction acts in tangential direction $\vec{n}_t$, which is chosen as the direction of the intersection points P_1, P_2 of the polygons. This

defines the direction $\vec{n}_n$, along which normal forces are acting. The force point from which the contact forces act on the particles is chosen as the center of mass S_{ij} of the overlap polygon. The velocity component resulting from the rotation of the particles ω_i, ω_j is computed with respect to this "contact point" S_{ij}. Additionally, damping in normal direction and friction in tangential direction is implemented.
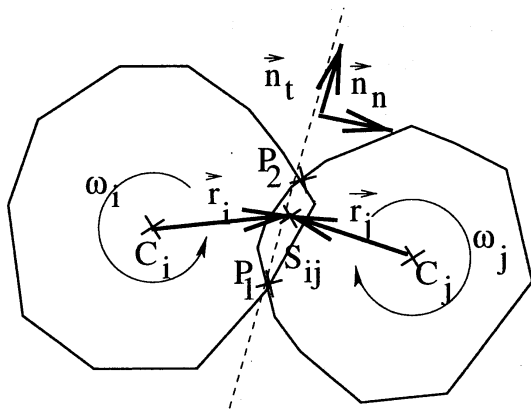
More details of the force law for the contact- and damping forces are explained in [11]. The simulation was performed for a two-dimensional system. We assumed that the cohesion strength is proportional to the contact area. Then, for two dimensions, the force is proportional to the contact length (dotted line in Fig. 21) whereas the repulsive force was chosen[11] proportional to the area overlap of two particles (shaded region in Fig. 21). For penetration spheres, the area overlap A and penetration depth x are proportional as $A \propto x^{3/2}$, so that the Hertz contact law $F \propto x^{3/2}$ for the contact force F is recovered. Likewise, for penetrating angles, the continuum mechanically correct contact law with $F \propto x^2$ is reproduced. No rolling friction was implemented, because no coefficients are available in the literature for granular materials, and in the presence of corners the normal dissipations dampens away rotations anyway.

Figure 20: Sketch of the contact situation for our polygonal collision law.

For the cohesion, the cohesion strength k_{coh} with units [N/m] in two dimensions is used, so that the attractive force F_{coh} is proportional to the contact length l:

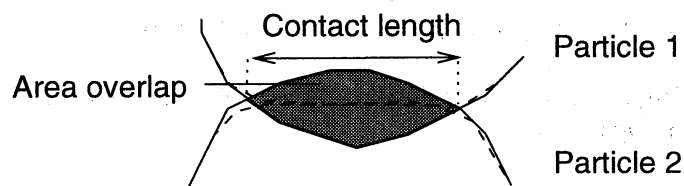$$F_{\text{coh}} = k_{\text{coh}} \cdot |l|, \tag{1}$$

Figure 21: Undeformed (full line) and deformed (dashed line) particles in a contact. The force resulting from the deformation is assumed to be proportional to the area overlap of the colliding particles. The penetration depth is exaggerated in comparison to simulations with realistic parameters.

In contrast to the model used in Ref. [31] for polygons, where the attractive force acts between the centers of mass of the particles, in our model the cohesive force acts at the contact points and depends on the length of the particle contact. The contact points are chosen as the center of the intersection points. Our definition of the cohesive force in Eq. 1 can be implemented easily in a simulation of polygons where the whole geometry of the contact is known. In the case of round particles, where only the penetration depth is computed, more complicated expressions are derived for the cohesion, see Ref. [32]. In our simulations, the average contact length (see Ref. [26]) of the particles increased linearly with the cohesion strength k_{coh}. The area of overlap of the particles increases also linearly.

In the simulation, the static and dynamic friction coefficients were chosen as $\mu_{stat.} = \mu_{dyn.} = 0.6$, Young's modulus was $Y = 10^7$ N/m, the particle radius was 0.00125 m for the particles. The time step for the simulations was dt=$0.2 \cdot 10^{-5}$ s, the density was 5000 kg/m^2.

All simulations used a flat ground with friction, but without any surface asperities. The pressures are computed using moving averages by computing the forces under line elements of 15 to 30 particle diameters of length. The effects were rather stable with respect to the natural fluctuations, the employed parameters and modified force laws.

References

[1] J.-P. Bouchaud, M. E. Cates, and P. Claudin, J. Phys. I **5**, 639 (1995).

[2] S. F. Edwards and C. C. Mounfield, Physica A **226**, 25 (1996).

[3] J.-P. Bouchaud, P. Claudin, M. E. Cates, and J. P. Wittmer, in *Physics of Dry Granular Media*, edited by H. J. Herrmann, J.-P. Hovi, and S. Luding (Kluwer Academic Publishers, Dordrecht, 1998), p. 97.

[4] S. Savage, in *Physics of dry granular media*, *ASI series*, NATO, edited by H. J. Herrmann, J.-P. Hovi, and S.Luding (Kluwer Academic Publishers, Cargese, 1998).

[5] F. H. Hummel and E. J. Finnan, Proc. Instn. Civil Engn. **212**, 369 (1921), the former: Minutes of Proc. of the Instn. of civil Engineers with other selected papers.

[6] T. Jotaki and R. Moriyama, Journal of the Society of Powder Technology, Japan **16**, 184 (1979).

[7] J. Šmid and J. Novosad, I. Chem. E. Symposium Series **63**, D3/V/1 (1981).

[8] R. Brockbank, J. M. Huntley, and R. Ball, J. Phys. II France **7**, 1521 (1997).

[9] I.K.Lee and J. Herrington, Proceedings of the first Australian-New Zealand Conference on Geomechanics: Melbourne **1**, 291 (1971).

[10] B. Lackinger, Ph.D. thesis, Mitteilungen des Instituts für Bodenmechanik, Felsmechanik und Grundbau an der Fakultät für Bauingenieurwesen und Architekture der Universität Innsbruck, 1980.

[11] H.-G. Matuttis, Granular Matter **1**, 83 (1998).

[12] L. Vanel, D. Howell, D. Clark, R. P. Behringer, and E. Clement, Phys. Rev. E **60**, R5040 (1999).

[13] K. Terzaghi, *Erdbaumechanik auf bodenphysikalischer Grundlage* (Frand Deuticke, Leipzig und Wien, 1925).

[14] Forchheimer, Zeitschrift der öst. I. u. A.-V (1882).

[15] Engesser, Deutsche Bauzeitung (1882).

[16] D. C. Hong, Phys. Rev. E **47**, 760 (1993).

[17] S. Luding, Phys. Rev. E **55**, 4720 (1997).

[18] D. H. Trollope and B. C. Burman, Géotechnique **30**, 137 (1980).

[19] G. Oron and H. J. Herrmann, Phys. Rev. E **58**, 2079 (1998), cond-mat/9707243.

[20] S. Luding and H.-G. Matuttis, in *Friction, Arching and Contact Dynamics*, edited by D. E. Wolf and P. Grassberger (World Scientific, Singapore, 1997), pp. 207–211.

[21] H.-G. Matuttis and S. Luding, in *Friction, Arching and Contact Dynamics*, edited by D. E. Wolf and P. Grassberger (World Scientific, Singapore, 1997).

[22] R. J. Bathurst and L. Rothenburg, J. Appl. Mech. **55**, 17 (1988).

[23] R. Albert, I. Albert, D. Hornbaker, P. Schiffer, and A.-L. Barabási, Phys. Rev. E **56**, R6271 (1997).

[24] D. J. Hornbaker, R. Albert, I. Albert, A.-L. Barabasi, and P. Schiffer, Nature **387**, 765 (1997).

[25] A. Schinner and H.-G. Matuttis, in *Traffic and Granular Flow '99*, edited by D. Helbing, H. J. Herrmann, M. Schreckenberg, and D. Wolf (Springer, Berlin, 2000), pp. 505–510.

[26] H.-G. Matuttis and A. Schinner, Journ. Mod. Phys. C **????**, ???? (2000).

[27] L.Bocquet, E.Charlaix, S.Ciliberto, and J.Crassous, Nature **396**, 745 (1998).

[28] R. L. Carr, Journ. Chem. Engin. **18**, 163 (1965).

[29] L. M. John M. Ting, Jeffrey D. Rowell, in *Proceedings on the 2nd International Conference on Discrete Element Methods (DEM)*, edited by J. R. Williams (IESL Publ., Cambridge, Mass, 1993), pp. 215–225.

[30] J. Šmid, P. V. Xuan, and J. Thýn, Chem. Eng. Technol. **16**, 114 (1993).

[31] F. Kun and H. J. Herrmann, Phys. Rev. E **59**, 2623 (1999).

[32] K. Johnson, K. Kendall, and A. Roberts, Proc. R. Soc. Lond. A **324**, 301 (1971).